Detecting Band Inversions by Measuring the Environment: Fingerprints of Electronic Band Topology in Bulk Phonon Linewidths

Kush Saha, Katherine Légaré, and Ion Garate
Département de Physique and Regroupement Québécois sur les Matériaux de Pointe, Université de Sherbrooke, Sherbrooke, Québec, Canada J1K 2R1

(Received 8 June 2015; published 23 October 2015)

The interplay between topological phases of matter and dissipative baths constitutes an emergent research topic with links to condensed matter, photonic crystals, cold atomic gases, and quantum information. While recent studies suggest that dissipative baths can induce topological phases in intrinsically trivial quantum materials, the backaction of topological invariants on dissipative baths is overlooked. By exploring this backaction for a centrosymmetric Dirac insulator coupled to phonons, we show that the linewidths of bulk optical phonons can reveal electronic band inversions. This result is the first known example where topological phases of an open quantum system may be detected by measuring the bulk properties of the surrounding environment.

DOI: 10.1103/PhysRevLett.115.176405 PACS numbers: 71.10.-w, 63.20.kd, 63.22.-m, 73.20.-r

Introduction.—The discovery of topological phases in three-dimensional crystals has culminated in a new classification scheme for solids that is based on quantum mechanics and topology [1]. These phases are described by integers known as topological invariants, which manifest themselves through robust gapless states localized at sample boundaries. The characterization of topological invariants in insulators often idealizes electrons as being isolated from their environment. Yet, in real materials, electrons are coupled to various nonelectronic baths and the usual idealization fails when the strength of the coupling exceeds the energy gap of the insulator.

Recent work [2,3] has suggested that baths can alter topological invariants and even induce topological phases. However, the inverse of this effect, concerning the backaction of topological invariants on baths, remains completely unexplored. Does a change in the electronic topological invariant modify the surrounding bath? Is it possible to infer the topological invariants of an electronic system by measuring its nonelectronic environment? The present work intends to answer these questions affirmatively and thus establish an unanticipated interplay between band topology and dissipative baths.

To that end, we adopt a minimal model that consists of massive 3D Dirac fermions coupled to a bath of phonons. In this model, we find that it is possible to learn whether the electronic band topology is trivial or nontrivial by analyzing the phonon linewidths in the thermodynamic limit (i.e., disregarding boundary effects). Our results challenge a commonly held viewpoint, according to which the bulk properties of a doped topological insulator and a doped trivial insulator should be qualitatively similar.

Model.—The minimal Hamiltonian describing the low-energy bulk bands of a time- and inversion-symmetric 3D Dirac insulator near the Brillouin zone center is [4]

$$\mathcal{H}(\mathbf{k}) = \gamma k^2 + \alpha \mathbf{k}\cdot\boldsymbol{\sigma}\tau^x + M_{\mathbf{k}}\tau^z, \tag{1}$$

where σ^i and τ^i are Pauli matrices in spin and orbital space (respectively), $\mathbf{k} = (k_x, k_y, k_z)$ is the crystal momentum, γ models the particle-hole asymmetry of the band structure, α is the Dirac velocity, $M_{\mathbf{k}} = m + \beta k^2$ is the Dirac mass, $2|m|$ is the energy gap of the insulator at $k = 0$, and β is an additional band parameter. Importantly, τ^z is the electronic parity operator and $[\tau^z, \mathcal{H}(\mathbf{0})] = 0$. For narrow-gap insulators described by Eq. (1), the sign of $m\beta$ determines the so-called strong topological invariant: if $\beta > 0$, then $m > 0$ ($m < 0$) results in a trivial (topological) insulator. If $m\beta < 0$, the electronic bands at $k = 0$ are said to be inverted. In addition, $M_{\mathbf{k}}$ acts as a momentum-dependent effective magnetic field that polarizes the orbital pseudospin $\boldsymbol{\tau}$ along the z direction. Because $M_{\mathbf{k}}$ changes sign as a function of k in the topological phase but not in the trivial phase, the k dependence of the expectation value of τ^z reflects the key difference between the bulk electronic structures of trivial and topological insulators [cf. Figs. 1(a) and 1(b)].

The eigenstates of Eq. (1) are $|u_{\mathbf{k}n}\rangle$, where $n \in \{1, \ldots, 4\}$ labels the two highest valence bands and the two lowest conduction bands near $k = 0$. The energy eigenvalues $E_{\mathbf{k}n}$ are doubly degenerate owing to the combined time-reversal and inversion symmetries. For analytical simplicity, we have chosen a continuum model with spherical symmetry; this captures the essential ideas and is smoothly deformable into more realistic lattice models that we use below for numerical calculations.

Phonon self-energy.—Electron-phonon interactions shift phonon frequencies and contribute to the phonon linewidth. These two effects can be calculated from the phonon self-energy [5]

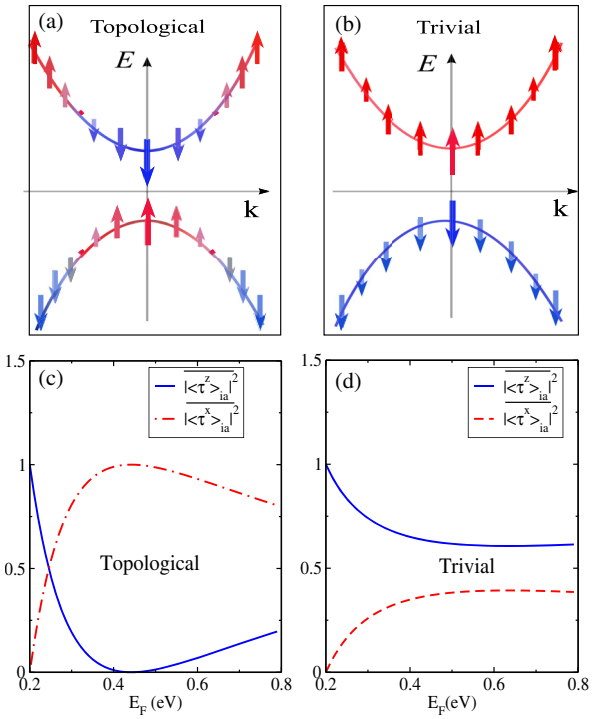

FIG. 1 (color online). (a),(b) Expectation value of the electronic parity operator $\langle\tau^z\rangle$ (represented by arrows) as a function of momentum for the electronic model of Eq. (1). (c),(d) Fermi surface averages of $|\langle\tau^z\rangle|^2$ and $|\langle\tau^x\rangle|^2$ [cf. Eq. (7)], as a function of the Fermi energy, for $m = -0.2$ eV (c) and $m = 0.2$ eV (d). The rest of the band parameters are the same as those in Ref. [3].

$$\Pi_\lambda(\mathbf{q},\omega_{\mathbf{q}\lambda}) = \frac{1}{\mathcal{V}}\sum_{\mathbf{k}nn'}\frac{|g^\lambda_{nn'}(\mathbf{k},\mathbf{q})|^2(f_{\mathbf{k}n}-f_{\mathbf{k}-\mathbf{q}n'})}{E_{\mathbf{k}n}-E_{\mathbf{k}-\mathbf{q}n'}-\omega_{\mathbf{q}\lambda}-i0^+}. \quad (2)$$

Here, $\mathcal{V}$ is the sample volume, λ labels different phonon modes, $\mathbf{q}$ is the phonon momentum, $\omega_{\mathbf{q}\lambda}$ is the bare phonon frequency, and $f_{\mathbf{k}n}$ is the fermion occupation number for the state $|u_{\mathbf{k}n}\rangle$ with a Fermi energy ϵ_F. Also,

$$g^\lambda_{nn'}(\mathbf{k},\mathbf{q}) = \langle u_{\mathbf{k}n}|\hat{g}^\lambda(\mathbf{q})|u_{\mathbf{k}-\mathbf{q}n'}\rangle, \quad (3)$$

where $\hat{g}^\lambda(\mathbf{q}) = \hat{g}^\lambda(-\mathbf{q})^\dagger$ is the electron-phonon vertex operator in the low-energy electronic subspace [6,9].

In a centrosymmetric crystal, lattice vibrations are either even or odd under spatial inversion. Each of these modes couples to electrons and can, as we shall see, inherit signatures of the underlying band topology. For the model of Eq. (1) and for $q \simeq 0$ optical phonons, inversion and time-reversal symmetries dictate [6]

$$\hat{g}^{\text{even}}(\mathbf{q}) \simeq g_0(\hat{\mathbf{q}}) + g_z(\hat{\mathbf{q}})\tau^z,$$
$$\hat{g}^{\text{odd}}(\mathbf{q}) \simeq g_x(\hat{\mathbf{q}})\tau^x + \mathbf{g}'(\hat{\mathbf{q}})\cdot\boldsymbol{\sigma}\tau^y, \quad (4)$$

where "even" ("odd") denotes the coupling of electrons to parity-even (parity-odd) phonon modes, with $[\hat{g}^{\text{even}},\tau^z] = 0$ and $\{\hat{g}^{\text{odd}},\tau^z\} = 0$. Inversion symmetry guarantees that $\hat{g}^{\text{even}}$ and $\hat{g}^{\text{odd}}$ will not be mixed in a single phonon mode. Also, $\hat{\mathbf{q}} = \mathbf{q}/q$, and the coefficients g_i $(i = 0, x, z)$ and g'_i $(i = x, y, z)$ can be obtained from the atomic displacements in the particular phonon mode [6]. Physically, g_0 and g_z lead to phonon-induced modulations of the chemical potential and the Dirac mass, respectively. Next, we identify ways in which $\hat{g}^\lambda$ can transfer the information about electronic band topology to the phonon sector.

Intraband phonon damping.—The main electronic mechanism contributing to phonon linewidths is the scattering of phonons off electron-hole pairs. The rate of this process is $\gamma^\lambda(\mathbf{q}) \equiv -\text{Im}\Pi_\lambda(\mathbf{q},\omega_{\mathbf{q}\lambda})$. In this work, we focus on long-wavelength optical phonons and on low temperatures.

We begin by considering the commonly realized case in which the phonon frequency is smaller than the band gap of the insulator. In this case, the "insulator" must be doped in order for carriers to absorb phonons and induce a linewidth γ^λ_{ia}. The subscript ia is shorthand for "intraband" and makes it explicit that phonons decay into particle-hole pairs in the vicinity of the Fermi surface. Assuming that the distance from the Fermi level to the bulk band edge is large compared to the phonon frequency, we have [6]

$$\gamma^\lambda_{ia}(q \simeq 0) \simeq \pi\omega_{\mathbf{0}\lambda}D(\epsilon_F)\overline{|g^\lambda_{ia}(\mathbf{k}_F,\hat{\mathbf{q}})|^2\delta(\mathbf{v}_F\cdot\mathbf{q}-\omega_{\mathbf{0}\lambda})}, \quad (5)$$

where $D(\epsilon_F)$ is the electronic density of states per band at the Fermi level, $\mathbf{k}_F$ is the Fermi wave vector, $\mathbf{v}_F$ is the Fermi velocity, $\delta(x)$ is the Dirac delta, and $|g^\lambda_{ia}(\mathbf{k},\hat{\mathbf{q}})|^2$ denotes the sum of $|g^\lambda_{nn'}|^2$ over the two degenerate bands at momentum $\mathbf{k}$ and energy $E_\mathbf{k}$ (hence the label intraband). In addition, $\bar{O} = \sum_\mathbf{k} O\delta(E_\mathbf{k}-\epsilon_F)/[\mathcal{V}D(\epsilon_F)]$.

Equation (5) contains information about the electronic band topology. The simplest way to see this is to imagine a parity-even phonon mode and a parity-odd phonon mode that couple to electrons purely through $\hat{g}^z \equiv g_z\tau^z$ and $\hat{g}^x \equiv g_x\tau^x$, respectively. More general couplings with $g_0 \neq 0$ and $g'_i \neq 0$ will be discussed below. From Eqs. (1), (3), and (5), the linewidths of these two phonon modes are [6]

$$\gamma^j_{ia}(q \simeq 0) \simeq |g_j(\hat{\mathbf{q}})|^2 D(\epsilon_F)\overline{|\langle\tau^j\rangle_{ia}|^2}\frac{\pi\eta}{2}\Theta(1-\eta), \quad (6)$$

where $j \in \{x,z\}$, $\Theta(x)$ is the Heaviside function, $\eta \equiv \omega_{\mathbf{0}j}/(qv_F)$, and

$$\overline{|\langle\tau^z\rangle_{ia}|^2} = 1 - \overline{|\langle\tau^x\rangle_{ia}|^2} = M^2_{k_F}/(\alpha^2k_F^2 + M^2_{k_F}). \quad (7)$$

Note that $\overline{|\langle\tau^j\rangle_{ia}|^2} \in [0,1]$ (cf. Fig. 1). In particular, when $M_{k_F} = 0$, $\overline{|\langle\tau^z\rangle_{ia}|^2} = 0$, and $\overline{|\langle\tau^x\rangle_{ia}|^2} = 1$. Combining Eqs. (6) and (7) with Fig. 1, it follows that γ^j_{ia} reflects the orbital texture, and therefore the topology, of the bulk bands. In order to clarify this point, we eliminate the

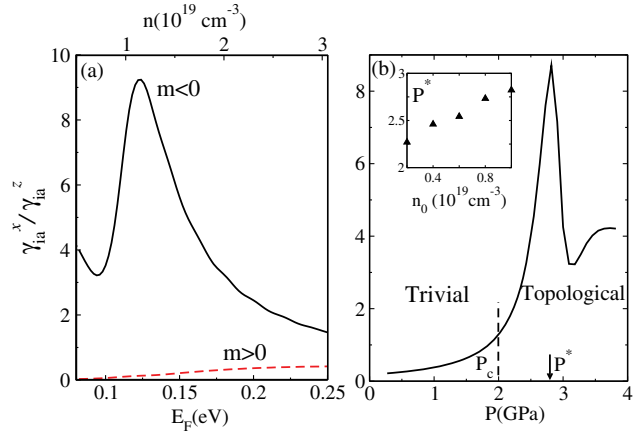

FIG. 2 (color online). (a) $\gamma^x_{ia}/\gamma^z_{ia}$ as a function of the Fermi energy and the bulk carrier density, for $m = \pm 0.1$ eV. A prominent maximum emerges in the topological phase only, due to the momentum-space orbital texture of the electronic eigenstates. (b) $\gamma^x_{ia}/\gamma^z_{ia}$ as a function of pressure P. We use $m = \alpha(P - P_c)$, where P_c is the critical pressure for a band inversion and α is a coefficient that can be obtained, e.g., from experiment [10]. The bulk carrier density is $n \simeq n_0(1 + P/B)$, where n_0 is the density at $P = 0$ and B is the bulk modulus. The maximum of $\gamma^x_{ia}/\gamma^z_{ia}$ appears at $P = P^*$. Inset: the dependence of P^* on n_0. As n_0 decreases, P^* approaches P_c, making it more difficult to identify trivial and topological phases solely from phonon measurements. Throughout this figure, we have used a tetragonal lattice regularization of Eq. (1). Because α, β, γ are not tabulated for Sb_2Se_3, we have replaced them with those of Sb_2Te_3 [4]. For the bulk modulus, we have used $B = 30$ GPa [11].

nontopological features coming from $D(\epsilon_F)$ by considering the ratio $\gamma^x_{ia}/\gamma^z_{ia} \simeq (g_x^2/g_z^2)\overline{|\langle\tau^x\rangle_{ia}|^2}/\overline{|\langle\tau^z\rangle_{ia}|^2}$.

For a fixed band gap, Eq. (6) predicts a strong maximum for $\gamma^x_{ia}/\gamma^z_{ia}$ as a function of ϵ_F in the topological phase (but not in the trivial phase) because M_{k_F} crosses zero as a function of ϵ_F in the topological phase (but not in the trivial phase). This difference in behavior between the trivial and topological phases is significant for a sizable $|m|$, but becomes gradually weaker as the energy gap decreases, ultimately disappearing when $m \to 0$. In other words, $\gamma^x_{ia}/\gamma^z_{ia}$ contains no signatures of band topology near the topological quantum critical point. Figure 2(a) confirms our analytical statements in a lattice model, for which Eq. (5) is solved numerically.

Alternatively, in a sample with fixed carrier density, $\gamma^x_{ia}/\gamma^z_{ia}$ shows a pronounced maximum as a function of m in the topological phase only. The maximum takes place at $m^* \simeq -\beta k_F^2$, where M_{k_F} undergoes a sign change. Motivated by recent claims of pressure-induced band inversions in Sb_2Se_3 and $Pb_{1-x}Sn_xSe$ [10,12], in Fig. 2(b) we plot $\gamma^x_{ia}/\gamma^z_{ia}$ as a function of pressure, using a lattice model. This corroborates the emergence of a "topology-induced" maximum in $\gamma^x_{ia}/\gamma^z_{ia}$.

In the preceding discussion of γ^x_{ia}, we have assumed a parity-odd phonon mode that couples to electrons purely through τ^x [$g'_i = 0$ in Eq. (4)]. In general, such a phonon can also couple to electrons through the term $\mathbf{g}' \cdot \boldsymbol{\sigma}\tau^y$. However, we have verified that this coupling produces qualitatively similar features as τ^x.

Similarly, when discussing γ^z_{ia}, we have imagined a parity-even phonon mode that couples to electrons purely through τ^z [$g_0 = 0$ in Eq. (4)]. Nonetheless, symmetry allows a mixture of τ^z and the identity matrix $\mathbf{1}$ [13]. The latter produces intraband matrix elements that are insensitive to the orbital texture of the insulator, since $\langle u_{\mathbf{k}n}|\mathbf{1}|u_{\mathbf{k}n}\rangle = 1$. Consequently, the effect of $g_0 \neq 0$ is to dilute away the topological features of γ^z_{ia}. Although this constitutes a problem towards the realization of Fig. 2 in real materials, we find that the maximum in $\gamma^x_{ia}/\gamma^z_{ia}$ remains pinned to the topological side if $|g_z| > |g_0|$.

Interband phonon damping.—Thus far, we have considered the linewidths of phonons with $\omega_{\mathbf{0}\lambda} < 2|m|$. Herein, we investigate the case $\omega_{\mathbf{0}\lambda} > 2|m|$, relevant to Dirac insulators with particularly small band gaps and/or high-frequency phonon modes. In this case, a phonon is absorbed by an electron in the bulk valence band, which gets promoted to the bulk conduction band. The associated phonon linewidth is γ^λ_{ie}, where the subscript *ie* is shorthand for "interband." Assuming for the moment that ϵ_F is inside the bulk gap, Eq. (2) yields [6]

$$\gamma^\lambda_{ie}(q \simeq 0) \simeq \pi D_{\text{joint}}(\omega_{\mathbf{0}\lambda})\overline{|g^\lambda_{ie}(\mathbf{k}, \hat{\mathbf{q}})|^2}, \tag{8}$$

where $D_{\text{joint}}(\omega) = \sum_{\mathbf{k}} \delta(E_{\mathbf{k}c} - E_{\mathbf{k}v} - \omega)/\mathcal{V}$ is the joint density of states, $E_{\mathbf{k}c}$ and $E_{\mathbf{k}v}$ are the bulk conduction (c) and valence (v) band energies. In addition, $|g^\lambda_{ie}|^2 = \sum_{n\in c, n'\in v}|g^\lambda_{nn'}|^2$ and $\overline{|g^\lambda_{ie}|^2} = \sum_{\mathbf{k}}|g^\lambda_{ie}|^2\delta(E_{\mathbf{k}c} - E_{\mathbf{k}v} - \omega_{\mathbf{0}\lambda})/(\mathcal{V}D_{\text{joint}})$.

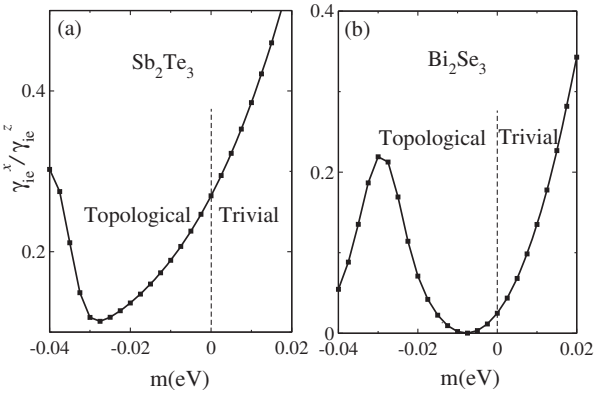

FIG. 3. $\gamma^x_{ie}/\gamma^z_{ie}$ as a function of the Dirac mass m, where the rest of the band parameters correspond to Sb_2Te_3 (a) or Bi_2Se_3 (b). The minimum of $\gamma^x_{ie}/\gamma^z_{ie}$ occurring in the topological side is a direct manifestation of the orbital texture in Fig. 1. Throughout this figure, we have used a tetragonal lattice regularization of Eq. (1) with the band parameters taken from Ref. [4]. The Fermi level is assumed to be inside the bulk gap.

From Eqs. (1) and (3), we obtain $|g^z_{ie}(\mathbf{k},0)|^2 = |g^x_{ia}(\mathbf{k},0)|^2$ and $|g^x_{ie}(\mathbf{k},0)|^2 = |g^z_{ia}(\mathbf{k},0)|^2$. Therefore, γ^λ_{ie} is as sensitive as γ^λ_{ia} to the band topology of the Dirac insulator (with x and z interchanged). More so, an important advantage of γ^λ_{ie} over γ^λ_{ia} is that we may effectively take $\hat{g}^{\text{even}} = \hat{g}^z$ regardless of the value of g_0 in Eq. (4), because $\langle u_{\mathbf{k}n}|\mathbf{1}|u_{\mathbf{k}n'}\rangle = 0$ for interband transitions. Accordingly, the topological signatures in γ^λ_{ie} are more robust than those in γ^λ_{ia}.

In a sample with fixed carrier density, $\gamma^x_{ie}/\gamma^z_{ie}$ contains a minimum as a function of m at $m^* \simeq -\omega_0^2\beta/(4\alpha^2)$, i.e., only in the topological phase [14]. This result has the same origin as the maximum of $\gamma^x_{ia}/\gamma^z_{ia}$ discussed above, and it holds for doped samples as well so long as $\alpha k_F/\omega_0 \ll 1$. Figure 3 confirms this for a lattice model.

Discussion.—In sum, there are three reasons why the linewidths of bulk, long-wavelength optical phonons can inherit distinct signatures of the electronic band topology. First, phonon linewidths are proportional to the square of energy-resolved electron-phonon matrix elements. Second, in a centrosymmetric crystal, the coupling of an optical $q \simeq 0$ phonon to electrons either commutes or anticommutes with the electronic parity operator. Third, the momentum-space texture of electronic parity eigenvalues reflects band inversions.

To be precise, the predicted features in the phonon linewidths probe band inversions near the Fermi level, rather than the strong topological invariant *per se*. However, in materials whose low-energy bands are described by Eq. (1), the energy gap minimum occurs at a single time-reversal-invariant momentum (TRIM) and hence a band inversion taking place therein is equivalent to a change in the strong topological invariant. By extension, phonon linewidths can probe the strong topological invariant in centrosymmetric crystals where the direct band gap minimum is known to occur at an odd number of symmetry-equivalent TRIMs. In contrast, phonon linewidths do not faithfully reflect the strong topological invariant in materials where the direct band gap minimum can occur at an even number of symmetry-equivalent TRIMs, or in materials lacking an inversion center.

Phonon frequencies, which we have barely mentioned thus far, are much less sensitive than phonon linewidths to the electronic band topology. This is because the real part of Eq. (2) contains a sum over electron-phonon matrix elements at multiple energies, with weights that depend on nontopological details of the energy bands. This notwithstanding, a recent experiment [10] in Sb_2Se_3 has attributed a kink in the pressure dependence of the phonon frequency to a band inversion. Our calculations [6] do not support such an interpretation.

The main tools to measure $q \simeq 0$ phonon linewidths are Raman spectroscopy (for parity-even phonons), infrared spectroscopy (for parity-odd phonons), and inelastic neutron scattering [15]. In a clean material with $\omega_{\mathbf{0}\lambda}\tau \gg 1$ (where τ is the disorder scattering time), γ^λ_{ia} vanishes unless $q > \omega_{\mathbf{0}\lambda}/v_F$ [16]. Since $\omega_{\mathbf{0}\lambda}/v_F$ typically exceeds the photon wave vector used in optical spectroscopies, γ^λ_{ia} should be measured with neutrons. In contrast, γ^λ_{ie} remains nonzero at $q = 0$ and is thus amenable to optics. For Bi_2Se_3, we estimate $\gamma^\lambda_{\text{ie,ia}} \lesssim 1\ \text{cm}^{-1}$, which nears the experimental resolution [17].

Aside from electron-phonon interactions, anharmonic lattice effects contribute to the phonon linewidth. To leading order, phonon-phonon interactions contain no information about the electronic band topology and are independent of the carrier density. Therefore, the anharmonic part can be subtracted by measuring the linewidths with respect to a baseline carrier density.

In view of our results, it is natural to ask whether any other physical observable involving Fermi's "golden rule," such as conductivity, might be sensitive to electronic band topology on the same footing as the phonon linewidths. The answer is generally negative. For example, the optical conductivity cannot clearly differentiate between trivial and nontrivial orbital textures in the bulk because the velocity operator mixes $\mathbf{1}$, τ^x, and τ^z [18].

To conclude, we have proven that it is in principle possible to infer the strong topological invariant of multiple Dirac insulators from the linewidths of bulk, long-wavelength optical phonons. It may be of interest to investigate formal links between the phonon linewidth and the SU(2) Berry phase identified in Ref. [19]. Likewise, it will be desirable to complement our theory with *ab initio* electronic structure calculations, and to search for similar insights in other contexts (cold atoms, photonic crystals, quantum memories) where the interplay between topology and dissipation may be crucial.

We are grateful to K. Pal and U. Waghmare for sharing useful information about Ref. [10]. This work has been funded by Québec's RQMP and Canada's NSERC. The numerical calculations were performed on computers provided by Calcul Québec and Compute Canada.

[1] See, e. g., *Topological Insulators*, Contemporary Concepts of Condensed Matter Science Vol. 6, edited by M. Franz and L. Molenkamp (Elsevier, Amsterdam, 2013).
[2] C.-E. Bardyn, M. A. Baranov, C. V. Krauss, E. Rico, A. Imamoglu, P. Zoller, and S. Diehl, New J. Phys. **15**, 085001 (2013).
[3] I. Garate, Phys. Rev. Lett. **110**, 046402 (2013); K. Saha and I. Garate, Phys. Rev. B **89**, 205103 (2014).
[4] C.-X. Liu, X.-L. Qi, H. J. Zhang, X. Dai, Z. Fang, and S.-C. Zhang, Phys. Rev. B **82**, 045122 (2010).
[5] See, e. g., T. Ando, J. Phys. Soc. Jpn. **75**, 124701 (2006).
[6] See Supplemental Material at http://link.aps.org/supplemental/10.1103/PhysRevLett.115.176405, which includes Refs. [7] and [8], for detail derivations of Eqs. (4–8) and related discussions.

[7] P. B. Allen and M. Cardona, Phys. Rev. B **23**, 1495 (1981).
[8] F. Szmulowicz, Phys. Rev. B **28**, 5943 (1983); G. L. Bir and G. E. Pikus, *Symmetry and Strain-Induced Effects in Semiconductors* (Wiley, New York, 1974).
[9] We consider only spatially local electron-phonon interactions, which means that $\hat{g}^{\lambda}(\mathbf{q})$ is independent of the electronic momentum $\mathbf{k}$. Hence, the entire $\mathbf{k}$ dependence of $g^{\lambda}_{nn'}(\mathbf{k},\mathbf{q})$ in Eq. (3) originates from $|u_{\mathbf{k}n}\rangle$. The neglect of nonlocal electron-phonon interactions is justifiable when k is small compared to the size of the Brillouin zone [6].
[10] A. Bera, K. Pal, D. V. S. Muthu, S. Sen, P. Guptasarma, U. V. Waghmare, and A. K. Sood, Phys. Rev. Lett. **110**, 107401 (2013).
[11] I. Efthimiopoulos, J. Zhang, M. Kucway, C. Park, R. C. Ewing, and Y. Wang, Sci. Rep. **3**, 2665 (2013).
[12] X. Xi, X.-G. He, F. Guan, Z. Liu, R. D. Zhong, J. A. Schneeloch, T. S. Liu, G. D. Gu, X. Du, Z. Chen, X. G. Hong, W. Ku, and G. L. Carr, Phys. Rev. Lett. **113**, 096401 (2014).
[13] Particle-hole symmetry, which could distinguish between $\mathbf{1}$ and τ^{z}, is broken in real Dirac insulators.
[14] For simplicity, we have assumed that the parity-odd and the parity-even mode under consideration have a similar frequency ω_0. When this assumption fails, our theory predicts a minimum of $\gamma^{x}_{ie}/D_{joint}(w_{\mathbf{0}x})$ at $m^{*} \simeq -\omega^{2}_{\mathbf{0}x}\beta/(4\alpha^{2})$, and a maximum of $\gamma^{z}_{ie}/D_{joint}(w_{\mathbf{0}z})$ at $m^{*} \simeq -\omega^{2}_{\mathbf{0}z}\beta/(4\alpha^{2})$.
[15] See, e. g., P. Y. Yu and M. Cardona, *Fundamentals of Semiconductors*, 4th ed. (Springer, Berlin, 2010).
[16] In practice the condition $q > \omega_{\mathbf{0}\lambda}/v_F$ is often compatible with long-wavelength phonons. For example, if $\omega_{\mathbf{0}\lambda} \simeq 100\ \mathrm{cm}^{-1}$ and $v_F \simeq 5 \times 10^{5}$ m/s, $\omega_{\mathbf{0}\lambda}/v_F \lesssim 0.005\ \text{Å}^{-1}$.
[17] S. M. Shapiro, G. Shirane, and J. D. Axe, Phys. Rev. B **12**, 4899 (1975); X. Zhu, L. Santos, C. Howard, R. Sankar, F. C. Chou, C. Chamon, and M. El-Batanouny, Phys. Rev. Lett. **108**, 185501 (2012); K. M. F. Shalil, M. Z. Hossain, V. Goyal, and A. A. Balandin, J. Appl. Phys. **111**, 054305 (2012); Y. Kim, X. Chen, Z. Wang, J. Shi, I. Miotkowski, Y. P. Chen, P. A. Sharma, A. L. Lima Sharma, M. A. Hekmaty, Z. Jiang, and D. Smirnov, Appl. Phys. Lett. **100**, 071907 (2012).
[18] In finite-sized samples, however, signatures of chiral surface states have been reported in the optical conductivity; see, e.g., V. Gnezdilov, Y. G. Pashkevich, H. Berger, E. Pomjakushina, K. Conder, and P. Lemmens, Phys. Rev. B **84**, 195118 (2011). It is not obvious that optical conductivity can distinguish between topological and trivial (Rashba-like) surface states.
[19] P. Hosur, P. Ghaemi, R. S. K. Mong, and A. Vishwanath, Phys. Rev. Lett. **107**, 097001 (2011).